Sixth International Symposium on Turbulence and Shear Flow Phenomena
Seoul, Korea, 22-24 June 2009

LARGE EDDY SIMULATION OF FLOW OVER A THREE-DIMENSIONAL MODEL VEHICLE

Jungil Lee
School of Mechanical and Aerospace Engineering,
Seoul National University
Seoul 151-744, Korea
deliciousair@empal.com

Haecheon Choi
School of Mechanical and Aerospace Engineering,
Seoul National University
Seoul 151-744, Korea
choi@snu.ac.kr

ABSTRACT

In the present study, large eddy simulations of turbulent flow over a three-dimensional model vehicle are conducted at Re=170,000 based on the vehicle height and free-stream velocity using an immersed boundary method (Kim *et al.*, 2001). As subgrid-scale models, we use the Smagorinsky model (SM; Smagorinsky, 1963) and a dynamic Vreman model (DVM; Park *et al.* 2006), respectively. The results of simulations are compared with those of an experiment by Khalighi *et al.* (2001). It is shown that results from DVM show good agreements with the experimental ones while SM results in poor predictions. Instantaneous flow fields are observed and it is found that an arch-like vortical structure exists in the near-wake of the vehicle. Also, we examine the flow statistics around the vehicle.

INTRODUCTION

Turbulent flow over a ground vehicle shows various phenomena such as the turbulent boundary layer, separation, shear layer and wake. The flow is complex and fully three-dimensional. Understanding the flow characteristics associated with the ground vehicle has a considerable practical significance because they are closely related to the aerodynamic performance of vehicle such as the drag and lift forces on the vehicle, acoustic noise, driving stability, etc. Therefore, many experimental and numerical studies have been conducted so far.

The experimental studies on the flow over a vehicle have been served as a primary research tool for understanding the aerodynamics of a ground vehicle. Especially, experimental studies with simplified vehicle models such as Ahmed model (Ahmed *et al.*, 1984) and GM model (Han *et al.*, 1996) have provided flow statistics and knowledge of flow structures in the wake.

Although early computational studies on the flow over a vehicle used the Reynolds-averaged Navier-Stokes (RANS) equation due to its low computational cost (Han, 1989), the advance of supercomputing technologies has made it possible to conduct large eddy simulations (LES) of flow over a vehicle at high Reynolds numbers (Verzicco *et al.*, 2002; Krajnovic and Davidson, 2005; Minguez *et al.*, 2008). From these studies using LES, detailed flow characteristics and highly unsteady nature of the flow have been examined.

In the present study, we conduct large eddy simulations of flow over a three dimensional model vehicle to examine the statistics and dynamics around the model vehicle. The three-dimensional model vehicle considered in this study is the GM model (Fig. 1). The GM model is a simplified three-dimensional model vehicle made by the General Motors. Also, we explore the applicability of dynamic Vreman model (DVM; Park *et al.*, 2006) which is a subgrid-scale (SGS) model developed for the large eddy simulation of complex flow.

COMPUTATIONAL DETAILS

Governing equations

The governing equations for the LES of flow around the three-dimensional model vehicle are the filtered continuity and incompressible Navier-Stokes equations:

$$\frac{\partial \overline{u}_i}{\partial x_i} - q = 0, \tag{1}$$

$$\frac{\partial \overline{u}_i}{\partial t} + \frac{\partial \overline{u}_i \overline{u}_j}{\partial x_j} = -\frac{\partial \overline{p}}{\partial x_i} + \frac{1}{Re_H}\frac{\partial^2 \overline{u}_i}{\partial x_j \partial x_j} - \frac{\partial \tau_{ij}}{\partial x_j} + f_i, \tag{2}$$

where $\mathbf{x} = (x_1, x_2, x_3) = (x, y, z)$ is the Cartesian coordinates, $\overline{\mathbf{u}} = (\overline{u}_1, \overline{u}_2, \overline{u}_3) = (u, v, w)$ is the filtered velocity, $\overline{p}$ is the filtered pressure, and Re_H denotes the Reynolds number based on the free stream velocity u_∞ and the vehicle height H. The subscripts 1, 2, 3 for the velocity and the coordinate denote the streamwise, transverse and spanwise directions, respectively. $\tau_{ij} = \overline{u_i u_j} - \overline{u}_i \overline{u}_j$ is the SGS stress tensor. q and f_i are the mass source/sink and the momentum forcing for the immersed boundary (IB) method suggested by Kim *et al.* (2001), respectively. The Reynolds number is $Re_H = 170,000$, at which Khalighi *et al.* (2001) conducted an experiment on the flow around the GM model.

Numerical methods and computational setup

For the time integration of the filtered Navier-Stokes equation, Eq. (2), a fully implicit time advancement (Crank-Nicolson scheme) is applied by utilizing a linearization of the convection term (Beam and Warming, 1978) and the velocity decoupling procedure (Kim *et al.*, 2002). For the spatial discretization, we use a hybrid scheme (Yun *et al.*, 2006)

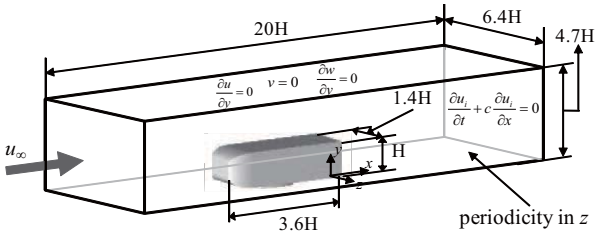

Figure 1: Schematic diagram of the computational domain, coordinate system and boundary conditions for LES of flow around the GM model.

combining an upwind scheme in the laminar flow region near the vehicle front to prevent the dispersion error caused by the central difference scheme, with the second-order central difference scheme in turbulent flow region. Since the adoption of third-order compact upwind difference scheme (CUDZ3; Zhong, 1998) used by Yun *et al.* (2006) causes numerical instabilities for the present computation, we use a third-order QUICK scheme (Leonard, 1979) as an upwind scheme. QUICK scheme is applied in $x/H < -2.9$ since Yi (2007) experimentally observed that the flow separates after the vehicle front and develops into turbulent boundary layer ($x = 0$ is the location of vehicle base).

Fig. 1 shows the schematic diagram of computational domain, coordinate system and boundary conditions used in this study. The computational domain is $-9 \le x/H \le 11$, $0 \le y/H \le 4.7$, and $-3.2 \le z/H \le 3.2$. At the inlet, a uniform free-stream velocity condition is imposed. At the outlet, a convective boundary condition $((\partial u_i/\partial t) + c(\partial u_i/\partial x) = 0)$ is used, where c is taken to be the mean exit velocity. At the freestream, a Neumann condition ($\partial u/\partial y = 0$, $v = 0$, and $\partial w/\partial y = 0$) is used and the no-slip condition is imposed at the bottom wall. The periodic boundary condition is imposed in the spanwise direction. The no-slip condition on the GM model surface is realized by the IB method (Kim *et al.*, 2001). The number of grid points is $545(x) \times 201(y) \times 245(z)$. As shown in Fig. 2, the computational mesh is clustered near the GM model and in the wake.

Simulations are carried out with the computational time step of $0.001H/u_\infty$. Data are averaged over 80 nondimensional time units after initial transient period to obtain the statistics.

SGS models

One of the objectives of the present study is to explore the applicability of DVM to LES of complex flows. For this purpose, we also conduct LES with the Smagorinsky model (SM; Smagorinsky, 1963) to compare the results with those from DVM. Note that, in principal, the dynamic Smagorinsky model (DSM; Germano *et al.*, 1991; Lilly, 1992) is not applicable to the present study since there is no statistically homogeneous direction for the averaging of model constant.

DVM and SM are the eddy viscosity models which assume that the SGS stress τ_{ij} is aligned with the strain rate tensor $S_{ij} = (1/2)(\partial u_i/\partial x_j + \partial u_j/\partial x_i)$. The eddy viscosity model for τ_{ij} is written in the following form:

$$\tau_{ij} - \frac{1}{3}\tau_{kk}\delta_{ij} = -2\nu_T \overline{S}_{ij}, \tag{3}$$

where ν_T is the turbulent eddy viscosity.

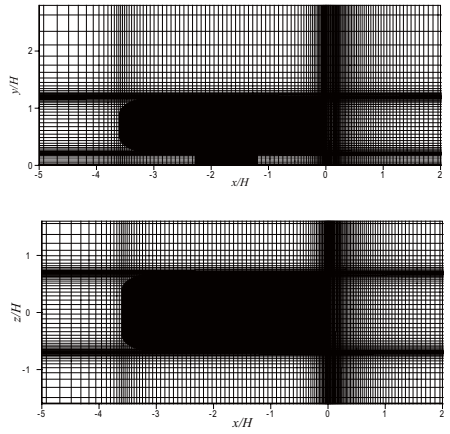

Figure 2: Grid distribution near the GM Model: (a) in the xy plane; (b) in the xz plane (every 3rd grid is shown).

Smagorinsky model. SM has the following form:

$$\nu_T = C_S^2 \overline{\Delta}^2 |\overline{S}|, \tag{4}$$

$$|\overline{S}| = \sqrt{2\overline{S}_{ij}\overline{S}_{ij}}, \tag{5}$$

where $\overline{\Delta}$ is a length scale usually taken to be a local grid spacing. The model coefficient C_S is set to be 0.16 which is a theoretical value for the isotropic turbulence. In the present study, wall-damping function is not used.

Dynamic Vreman model. DVM utilizes the Vreman model (Vreman, 2004), which guarantees zero eddy viscosity for various laminar shear flows, as a base model. The formulation of the Vreman model is:

$$\nu_T = C_v \sqrt{\frac{II_{\overline{\beta}}}{\overline{\alpha}_{ij}\overline{\alpha}_{ij}}}, \tag{6}$$

$$\overline{\alpha}_{ij} = \frac{\partial \overline{u}_j}{\partial x_i}, \tag{7}$$

$$II_{\overline{\beta}} = \overline{\beta}_{11}\overline{\beta}_{22} + \overline{\beta}_{22}\overline{\beta}_{33} + \overline{\beta}_{33}\overline{\beta}_{11} - \overline{\beta}_{12}^2 - \overline{\beta}_{23}^2 - \overline{\beta}_{31}^2, \tag{8}$$

$$\overline{\beta}_{ij} = \sum_{m=1}^{3} \overline{\Delta}_m^2 \overline{\alpha}_{mi}\overline{\alpha}_{mj}, \tag{9}$$

where C_v is the model coefficient, and $\overline{\Delta}_m$ is the characteristic filter width in the mth direction. DVM dynamically adjusts the model coefficient C_v according to the flow based on the Germano identity (Germano *et al.* 1991), and C_v has the form:

$$C_v = -\frac{1}{2}\frac{\langle L_{ij}M_{ij}\rangle_V}{\langle M_{ij}M_{ij}\rangle_V}, \tag{10}$$

where

$$L_{ij} = \widetilde{\overline{u}_i\overline{u}_j} - \widetilde{\overline{u}}_i\widetilde{\overline{u}}_j, \tag{11}$$

$$M_{ij} = \sqrt{\frac{II_{\widetilde{\overline{\beta}}}}{\widetilde{\overline{\alpha}}_{ij}\widetilde{\overline{\alpha}}_{ij}}}\widetilde{\overline{S}}_{ij} - \sqrt{\widetilde{\frac{II_{\overline{\beta}}}{\overline{\alpha}_{ij}\overline{\alpha}_{ij}}}}\overline{S}_{ij}, \tag{12}$$

$\langle\bullet\rangle_V$ denotes the instantaneous volume averaging in the entire computational domain, and $\widetilde{()}$ denotes the test-filtering operation. Note that C_v is globally constant in space and varies only in time; i.e., $C_v = C_v(t)$.

Table 1: Flow statistics from present simulations and the experiment conducted by Khalighi *et al.* (2001). ($\overline{C}_D$: time-averaged drag coefficient, $\overline{C}_L$: time-averaged lift coefficient, $\overline{C}_{P_b}$: time-averaged pressure coefficient at the vehicle base)

	$\overline{C}_D$	$\overline{C}_L$	$\overline{C}_{P_b}$	Remark
No SGS model	-	-	-	diverged
SM	0.353	-0.198	-0.267	-
DVM	0.324	-0.270	-0.247	-
Experiment	0.3	-	-0.226	-

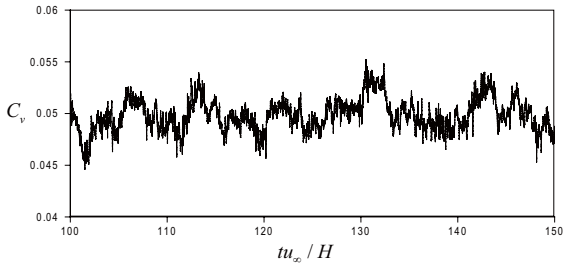

Figure 3: Temporal evolution of C_v for LES with DVM.

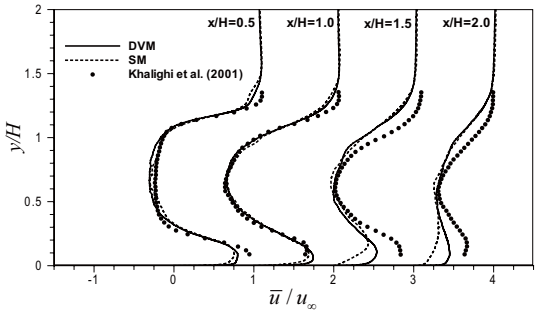

Figure 4: Time-averaged streamwise velocity profiles in an xy plane ($z/H = 0$).

RESULTS AND DISCUSSION

Evaluation of SGS models

In this section, we present the results from LES of flow around the GM model with DVM and SM. Also, a simulation without SGS model is attempted to evaluate the effect of the SGS models. However, the simulation without SGS model leads to numerical instabilities and eventually diverges. Thus, the use of SGS model is crucial for the present problem.

Table 1 summarizes some statistical quantities from the present simulations together with the experimental data by Khalighi *et al.* (2001). The time-averaged drag coefficient ($\overline{C}_D$), lift coefficient ($\overline{C}_L$) and pressure coefficient at the vehicle base ($\overline{C}_{P_b}$) from LES with DVM show good agreement with the experimental data. Fig. 3 shows the temporal evolution of C_v for LES with DVM. As shown, C_v is statistically stationary with time-averaged value of 0.05. Meanwhile, LES with SM shows some deviation from the experimental data.

Fig. 4 shows the time-averaged streamwise velocity profiles in an xy plane ($z/H = 0$) at four streamwise locations in the wake. At $x/H = 0.5$ and $x/H = 1.0$, results from both DVM and SM agree well with the experimental data. At $x/H = 1.5$ and $x/H = 2.0$, it is observed that results from

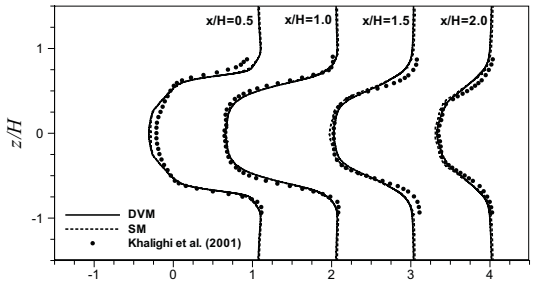

Figure 5: Time-averaged streamwise velocity profiles in an xz plane ($y/H = 0.7$).

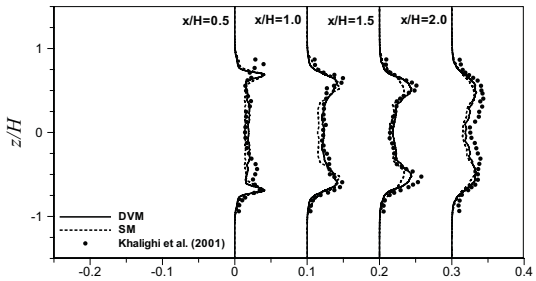

Figure 6: Resolved streamwise turbulence intensity profiles in an xz plane ($y/H = 0.7$).

DVM and SM show some deviation from the experiment in the shear layer and near the bottom wall. Near the bottom wall, there is a difference between the profiles from DVM and SM, and results from DVM show better agreement with the experiment.

Fig. 5 shows the time-averaged streamwise velocity profiles in an xz plane ($y/H = 0.7$) at four streamwise in the wake. At all the locations shown in Fig. 5, results from DVM and SM are quite similar and show excellent agreement with the experiment.

Fig. 6 shows resolved streamwise turbulence intensity profiles in an xz plane ($y/H = 0.7$) at four streamwise locations in the wake. Overall, results from DVM and SM agree with the experiment. However, the results from SM slightly underpredict the profiles at $x/H = 1.0$ and the peak values at $x/H = 1.5$ compared to the results from DVM and the experiment.

From the observation of the statistics in the wake, we can notice that LES with SM shows fairly reasonable results compared to the experimental data, although predicted statistics such as $\overline{C}_D$ and $\overline{C}_{P_b}$ are largely deviate from the experiment. To examine this inconsistency, we investigate the turbulent boundary layers on the GM model surface.

Fig. 7 shows the time-averaged streamlines on the upper surface of GM model in an xy plane ($z/H = 0$). As shown in Fig. 7, the flow separates on the vehicle front and reattaches on the vehicle surface. The predicted locations of reattachment from DVM and SM are $x/H = -2.59$ and $x/H = -2.13$, respectively, and are quite different. Also, the shapes of the recirculation bubble from both models are different. The differences between both models are again observed in the time-averaged streamwise velocity profiles above the upper surface of GM model shown in the Fig. 8. To elucidate this differences, eddy-viscosities from both models are shown in Fig. 9. The eddy viscosity from DVM smoothly converges to zero as it goes to the wall. However, it

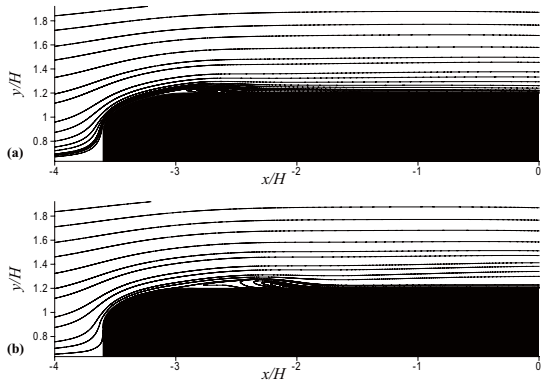

Figure 7: Time-averaged streamlines on the upper surface of GM model in an xy plane ($z/H = 0$): (a) DVM; (b) SM.

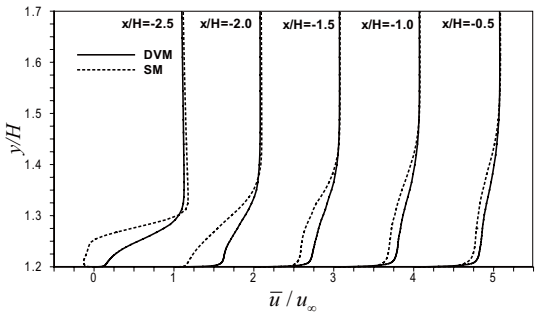

Figure 8: Time-averaged streamwise velocity profiles above the upper surface of GM model in an xy plane ($z/H = 0$).

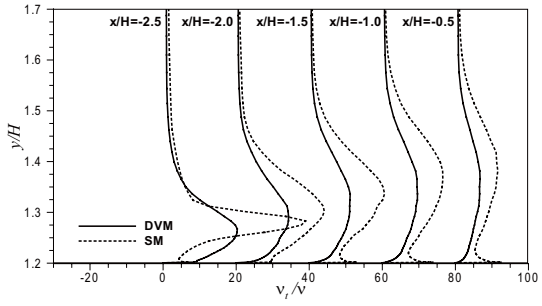

Figure 9: Time-averaged ratio of eddy-viscosity to molecular viscosity above the upper surface of GM model in an xy plane ($z/H = 0$).

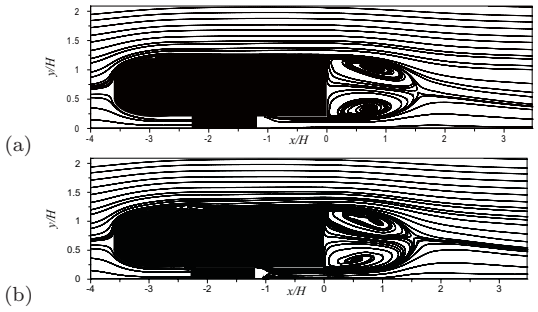

Figure 10: Time-averaged streamlines around GM model in an xy plane ($z/H = 0$): (a) DVM; (b) SM.

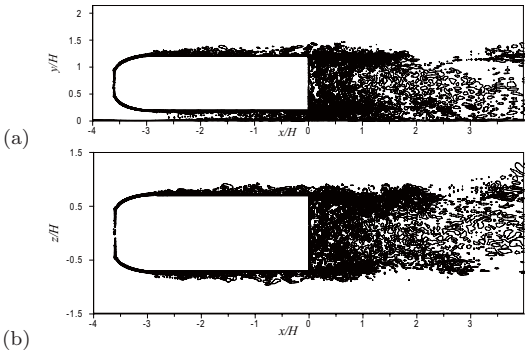

Figure 11: Instantaneous vorticity contours around GM model: (a) spanwise vorticity in an xy plane ($z/H = 0.2$); (b) transverse vorticity in an xz plane ($y/H = 0$).

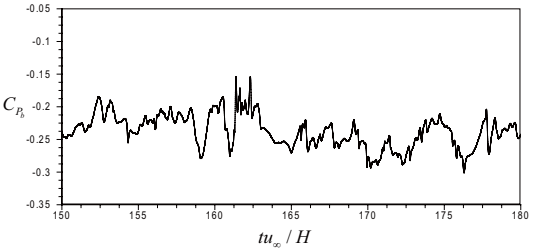

Figure 12: Time history of the pressure coefficient C_{P_b} at the base of GM model.

is observed that the eddy viscosity from SM does not asymptotically converge to zero near the wall, and predicts a high peak right above the wall. This unphysical behavior of SM may hinder the prediction of turbulent boundary layer near the vehicle surface. Fig. 10 shows time-averaged streamlines around GM model in an xy plane ($z/H = 0$). As mentioned above, a small separation bubble exists at the end of the curved surface of the vehicle front. Large recirculation bubbles are formed behind the vehicle. The length of the recirculation region predicted by the present simulation is about $1.5H$. Since DVM performs slightly better than SM, we hereinafter present results only from LES with DVM.

Instantaneous vorticity field

Fig. 11 shows the instantaneous vorticity contours around the GM model. The flow separates right after the curved surface of the vehicle front and immediately reattaches, forming small separation bubbles. This reattached flow develops into the turbulent boundary layer above the surface of the GM model. The main separation occurs at the trailing edge of the GM model. There is no shear layer transition to turbulence in the wake due to turbulent separation. The flow behind the vehicle contains many small-scale vortices. Especially, strong small-scale vortices are concentrated in the shear layer region, indicating large turbulence intensities there.

Instantaneous pressure field

Fig. 12 shows the time history of the pressure coefficient C_{P_b} at the base of GM model. The temporal evolution of C_{P_b} is highly unsteady, and its time-averaged value is -0.247, being in agreement with the experimental data (see Table 1).

Large-scale structures around the GM model are illustrated in Fig. 13 using the iso-surface of instantaneous

Figure 13: Iso-surface of instantaneous pressure fluctuation ($p'/\rho u_\infty^2 = -0.05$).

pressure fluctuation. Since the core of the vortical structures is closely related to the low pressure region, we set the iso-value of pressure fluctuation to be $p'/\rho u_\infty^2 = -0.05$. As shown in Fig. 13, complex three-dimensional flow structures exist behind the vehicle. In the near-wake region, an arch-like vortical structure appears intermittently and travels downstream losing their coherence.

CONCLUSIONS

In this study, we evaluated the performance of DVM for the prediction of flow over a GM model vehicle by comparing the results with the experimental data by Khalighi *et al.* (2001) and those from LES with SM. Before conducting LES, simulation without SGS model was attempted and the simulation diverged. The computed flow statistics by LES with DVM showed good agreement with the experimental data. On the other hand, although LES with SM showed fairly reasonable results in the wake, it provided relatively poor statistics possibly due to the poor prediction of turbulent boundary layers above the vehicle surface. In conclusion, present results from LES with DVM supports the applicability of DVM to the flow with a complex geometry where there is no homogeneous direction.

The incoming flow separated from and reattached on the front vehicle surface, forming a small recirculation bubble there, and developed into the turbulent boundary layers above the vehicle surface. In the near-wake of the vehicle, an arch-like vortical structure existed and traveled downstream.

ACKNOWLEDGEMENT

The financial support from the National Research Laboratory Program of Korean Ministry of Education, Science and Technology is gratefully acknowledged. Also, the authors would like to appreciate the use of the supercomputing system of the Supercomputing Center under "The 11th Strategic Supercomputing Support Program" from Korea Institute of Science and Technology Information.

REFERENCES

Ahmed, S. R., and Ramm, G., 1984, "Salient features of the time-averaged ground vehicle wake", *SAE Paper*, No. 840300.

Beam, R. M., and Warming., R.F., 1978, "An implicit factored scheme for the compressible Navier-Stokes equations", *AIAA Journal*, Vol. 16, pp. 393-402.

Germano, M., Piomelli, U., Moin, P., and Cabot, W. H., 1991 , "A dynamic subgrid-scale eddy viscosity model", *Physics of Fluids*, Vol. A 3, pp. 1760-1765.

Han, T., 1989, "Computational analysis of three-dimensional turbulent flow around a bluff body in ground proximity", *AIAA journal*, Vol. 27, pp. 1213-1219.

Han, T., Sumantran, V., Harris, C., Kuzmanov, T., Huebler, M., and Zak, T., 1996, "Flow-field simulations of three simplified vehicle shapes and comparisons with experimental measurements", *SAE transactions*, vol. 105, pp. 820-835.

Khalighi, B., Zhang, S., Koromilas, C., Balkanyi, S. R., Bernal, Luis P., Iaccarino, G., and Moin, P., 2001, "Experimental and computational study of unsteady wake flow behind a bluff body with a drag reduction Device", *SAE Paper*, 2001-01-1042.

Kim, J., Kim, D., and Choi, H., 2001, "An immersed boundary finite-volume method for simulations of flow in complex geometries", *Journal of Computational Physics*, Vol. 171, pp. 132-150.

Kim, K., Baek, S. J., and Sung, H. J., 2002, "An implicit decoupling procedure for the incompressible Navier-Stokes equations", *International Journal for Numerical Methods in Fluids*, Vol. 38, Issue 2, pp. 125-138.

Krajnovic, S., and Davidson, L., 2005, "Flow Around a Simplified Car, Part 1: Large Eddy Simulation", *Journal of Fluids Engineering*, Vol. 127, pp. 907-918.

Leonard, B. P., 1979, "A stable and accurate convective modeling procedure based on quadratic upstream interpolation", *Computer Methods in Applied Mechanics and Engineering*, Vol. 19, pp. 59-98.

Lilly, D., 1992, "A proposed modification of the Germano subgrid-scale closure method", *Physics of Fluids*, Vol. A 4, pp. 633-635.

Minguez, M., Pasquetti, R., and Serre, E., 2008, "High-order large-eddy simulation of flow over the "Ahmed body" car model", *Physics of Fluids*, Vol. 20, 095101.

Park, N., Lee, S., Lee, J., and Choi, H., 2006, "A dynamic subgrid-scale eddy viscosity model with a global model coefficient", *Physics of Fluids*, Vol. 18, 125109.

Smagorinsky, J., 1963, "General circulation experiments with primitive equations - I. The basic experiments", *Monthly Weather Review*, Vol. 91, pp. 99-164.

Verzicco, R., Fatica, M., Iaccarino, G., Moin, P., and Khalighi, B., 2002, "Large eddy simulation of a road vehicle with drag-reduction devices", *AIAA Journal*, Vol. 40, No. 12, pp. 2447-2455.

Vreman, A. W., 2004, "An eddy-viscosity subgrid-scale model for turbulent shear flow: Algebraic theory and applications", *Physics of Fluids*, Vol. 16, pp. 3670-3681.

Yi, W., 2007, "Drag reduction of a three-dimensional car model using passive control device", Ph. D. thesis, Seoul National University, Seoul, Korea

Yun, G., Kim, D., and Choi, H., 2006, "Vortical structures behind a sphere at subcritical Reynolds numbers", *Physics of Fluids*, Vol. 18, 015102.